# NECK INFLUENCE ON BINARY CONFIGURATION SHELL EFFECTS

R. A. GHERGHESCU

National Institute of Physics and Nuclear Engineering, RO-76900 Bucharest, Romania

*Received June 9, 2005*

A necked potential is studied, based on deformed oscillator wells in direct correspondance with the shape change of the nuclear system. For the first time a potential responsible for the necking part between the fragments is introduced on potential theory basis. As a direct consequence, spin-orbit **ls** and $\mathbf{l}^2$ operators are calculated as shape dependent. Level scheme evolution along the fission path for pairs of spheroidally deformed fragments is calculated. The Strutinsky method yields the shell corrections for different neck radii.

## 1. INTRODUCTION

The importance of an adequate description of cold fission, cluster radioactivities and alpha decay in terms of an asymmetric and *deformed* single particle shell model with more realistic shapes during fission and fusion processes was repeteadly stressed [1].

Recently, attempts have been made to use the two-center shell model in synthesis and decay of superheavy nuclei. It is a suitable theoretical model to study the microscopic effects on possible projectile-target combinations in their way from two different quantum systems to one. As the synthesized nucleus is heavier, increasing Coulombian repulsion lowers the macroscopic potential barrier almost to complete disappearance. The only way a superheavy element can survive is due to the shell effects [2]. A two-center shell model is essential for the description of fusion and fission of superheavy elements. It shows that the shell structure of the two participating target-projectile nuclei is visible far beyond the barrier into the fusioning nucleus and is crucial in choosing the most favorable pair approaching each other through *cold* fusion valleys. Transition behaviour of the two partner shells will provide shell corrections which lower the fusion barrier to be overcome, as compared to neighbouring projectile-target combinations.

Up to now, all the variants of two-center shell models used spherical nuclei. I shall consider now the motivation of this work. In any process which implies a pass from two quantum systems to one (fusion) or the other way around (fission) there are certain situations when one or both fission fragments

or fusion partners are deformed. Such a reaction could yield cold energy valleys due to deformed shell structure of the participants. Fragment deformations are properly accounted in this work. A deformed two-center shell model (DTCSM) is proposed, where the main part of the potential consists of two ellipsoidally deformed Nilsson type oscillators for axially symmetric shapes. Any change in the nuclear surface shape is reflected in a corresponding modification of the four oscillator frequencies along the symmetry axis and perpendicular to it.

It is also well established that, especially in fission and cluster decay, a necking region builds its way between the fragments, smoothly linking the two ellipsoids one to the other. This work associates for the first time a microscopic potential to a spherically matching neck region of the nuclear shape. The neck potential is constructed in such a way that it takes the same value on the necking region surface as on the ellipsoidal region surfaces of the fragments. Equipotentiality is thus respected on the nuclear surface.

The usual spin-orbit and squared angular momentum operators are calculated with the help of the potential-dependent formulae $\mathbf{ls} = (\nabla V \times \mathbf{p})\mathbf{s}$, and $\mathbf{l}^2 = (\nabla V \times \mathbf{p})^2$ [3]. The potential in this model follows exactly the nuclear shape, and so do the $\mathbf{ls}$ and $\mathbf{l}^2$ operators. Finally, the levels diagram with respect to the elongation, neck parameter and fragment deformations are used to calculate the shell correction by means of the Strutinsky method.

## 2. SHAPES

Two spheroids (the deformed fragments) with semiaxes $a_1$, $b_1$ and $a_2$, $b_2$ are, at a certain moment, separated at a distance $R$ between the two centers $O_1$ and $O_2$. A sphere centered in $O_3$ with radius $R_3$ is rolling around the symmetry axis, being tangent all the time to the two ellipsoids. The necking region, between the two tangent points, is generated in this way. Thus we have five independent parameters to design the deformation space: two fragment shape asymmetries $\chi_1 = b_1/a_1$, $\chi_2 = b_2/a_2$ (if $a_1$ and $a_2$ are given as the correspondent of $\beta_2$ for every $A_1$ and $A_2$, the other semiaxes are calculated from the total volume conservation condition), mass asymmetry $A_1/A_2$, the neck radius $R_3$ and the distance between centers $R$. Obviously, this set is available for every parent nucleus $A$, $Z$ with its own $\chi = b/a$.

## 3. THE POTENTIAL

The equations for shape surfaces described in the previous section can be written in cylindrical coordinates (due to axyal symmetry) as:

$$\rho(z)=\begin{cases}\rho_1(z)= & [b_1^2-\chi_1^2 z^2]^{1/2} & -a_1\le z\le z_{c1}\\ \rho_g(z)= & \rho_3-[R_3^2-(z-z_3)^2]^{1/2}, & z_{c1}\le z\le z_{c2}\\ \rho_2(z)= & [b_2^2-\chi_2^2(z-R)^2]^{1/2}, & z_{c2}\le z\le R+a_2\end{cases} \tag{1}$$

where the origin is placed in the center of the heavy fragment $O_1$. Neck sphere center coordinates are $(z_3,\rho_3)$, and $z_{c1}$ and $z_{c2}$ are the two tangent points of the neck sphere with the two ellipsoids.

The oscillator potential correspondig to these two-center shapes must have the same value on the nuclear surface. For spheres , for example, we have:

$$V_0=\frac{m_0\omega_i^2R_i^2}{2} \tag{2}$$

where $R_i$ is the radius of a nucleus with atomic mass $A_i$. Since $\hbar\omega_i=41A^{-1/3}$ and $R_i=r_0A^{1/3}$ (where $r_0\approx 1.16$) then $V_0\approx 54.5$ MeV. If we write these simple relations for the surface of ellipsoidal shapes:

$$\begin{aligned}\frac{1}{2}m_0\omega_{z_i}^2a_i^2&=V_0\\ \frac{1}{2}m_0\omega_{\rho_i}^2b_i^2&=V_0\end{aligned} \tag{3}$$

the frequencies $\omega_{z_i}$, $\omega_{\rho_i}$ are defined along the symmetry axis and respectively perpendicular to it, as functions of the two ellipse semiaxes.

For an arbitrary origin, placed on the symmetry axis, the ellipsoids surface equations read:

$$\begin{aligned}\frac{\rho^2}{\frac{2V_0}{m_0\omega_{\rho_1}^2}}+\frac{(z+z_1)^2}{\frac{2V_0}{m_0\omega_{z_1}^2}}&=1\\ \frac{\rho^2}{\frac{2V_0}{m_0\omega_{\rho_2}^2}}+\frac{(z-z_2)^2}{\frac{2V_0}{m_0\omega_{z_2}^2}}&=1\end{aligned} \tag{4}$$

where $z_1$ and $z_2$ are the absolute values of each of the two centers coordinates. Now the two oscillator potential expressions for deformed fragments come straightforward:

$$V_1(\rho,z)=\frac{1}{2}m_0\omega_{\rho_1}^2\rho^2+\frac{1}{2}m_0\omega_{z_2}^2(z+z_1)^2$$

$$V_2(\rho, z) = \frac{1}{2} m_0 \omega_{\rho_2}^2 \rho^2 + \frac{1}{2} m_0 \omega_{z_2}^2 (z - z_2)^2 \tag{5}$$

What we have left to establish is the necking region potential, $V_g(\rho, z)$. The force that keeps nucleons confined within the ellipsoid is an attractive type one, radially inward ($\vec{F}_{ellipsoid} \sim -\vec{r}$). The same reason leads us to the hypothesis that, if nucleons are confined within the concave necking region, which is geometrically *inversed* to the ellipsoid convex surface with respect to the centers of the fragments, a rejective force is needed, radially outward:

$$\vec{F}(\vec{r}) = -\beta \vec{r} \tag{6}$$

hence a force oriented from outside the nuclear shape toward the surface. Then the corresponding potential is related to the expression:

$$\int_0^r \vec{F} \mathrm{d}\vec{r} = \varphi(r) - \varphi(0) \tag{7}$$

or

$$\int_0^r \vec{F} \mathrm{d}\vec{r} = \int_0^r -\beta \vec{r} \mathrm{d}\vec{r} = -\frac{\beta r^2}{2} \tag{8}$$

Consequently, $\varphi(r) = -\frac{\beta r^2}{2}$ is a potential form generating the rejective force. In this way, the rejective neck potential, defined up to a constant, must look like:

$$V_{g1}(r) = V_c + \varphi(r) \tag{9}$$

where $V_c$ is a constant to be determined. On the nuclear surface $S_g$, we have again:

$$V_{g1}\Big|_{S_g} = V_c + \varphi(r)\Big|_{S_g} = V_0 \tag{10}$$

or

$$V_c = V_0 - \varphi(r)\Big|_{S_g} \tag{11}$$

For the sake of consistency, the rejective force is also considered of oscillator type:

$$\vec{F}(\vec{r}) = -m_0 \omega_g^2 \vec{r} \tag{12}$$

therefore

$$\varphi(r) = -\frac{m_0 \omega_g^2 r^2}{2} \tag{13}$$

where the frequency $\omega_g$ has to be found. Since the potential must follow the geometrical shape, at the neck region the function $\varphi(r) = \varphi(\rho, z)$ reads:

$$\varphi(\rho, z) = -\frac{m_0\omega_g^2}{2}[(\rho-\rho_3)^2 + (z-z_3)^2] \tag{14}$$

and is centered in the middle of the neck sphere $O_3(\rho_3, z_3)$. On the neck surface then, where $(\rho, z) \in S_g$, we have:

$$\varphi(\rho, z)\Big|_{S_g} = \frac{m_0\omega_g^2}{2}R_3^2 = V_{g1}\Big|_{S_g} = V_0 \tag{15}$$

Then $V_c = V_0 - \varphi(r)\Big|_{S_g} = 2V_0$ and the total neck potential from outside the shape down to the surface is:

$$V_{g1}(r) = 2V_0 - \frac{m_0\omega_g^2}{2}[(\rho-\rho_3)^2 + (z-z_3)^2] \tag{16}$$

and the neck frequency is directly related to the neck radius by Eq. (15). $V_{g1}$ reaches its maximum at the center of the neck sphere $(\rho = \rho_3, z = z_3)$, where $V_{g1} = 2V_0$, then is decreasing down to the surface value $V_{g1} = V_0$ at a distance equal to the neck radius $(\rho-\rho_3)^2 + (z-z_3)^2 = R_3^2$ from $O_3$.

To complete the neck-dependent potential, there still remains the region inside the nuclear shape between the necking surface and the interior contours of the two ellipsoids (black colored, denoted by $V_{g2}(\rho, z)$ in the upper part of Fig. 3). It can be observed that on the ellipsoids surface *inside* the shape the deformed oscillator potential has the same value as on the fragments surface, namely $V_0$. But on the surface of the shape within the necking region, the value is also $V_0$. Then, one concludes that inside the region volume between the neck surface and the two ellipsoids surfaces – $\rho_1(z) \le \rho \le \rho_g(z)$ and $\rho_2(z) \le \rho \le \rho_g(z)$ – the neck potential is constant.

$$V_{g2}(\rho, z) = cst = V_0 \tag{17}$$

Finally, the deformed oscillator potential part for the DTCSM reads:

$$V_{DTCSM}(\rho, z) = \begin{cases} V_1(\rho, z) = \frac{1}{2}m_0\omega_{\rho_1}^2\rho^2 + \frac{1}{2}m_0\omega_{z1}^2(z+z_1)^2 \\ V_g(\rho, z) = \begin{cases} V_{g1}(\rho, z) = 2V_0 - \left[\frac{1}{2}m_0\omega_g^2(\rho-\rho_3)^2 + \frac{1}{2}m_0\omega_g^2(z-z_3)^2\right] \\ V_{g2}(\rho, z) = V_0 \end{cases} \\ V_2(\rho, z) = \frac{1}{2}m_0\omega_{\rho_2}^2\rho^2 + \frac{1}{2}m_0\omega_{z_2}^2(z-z_2)^2 \end{cases} \tag{18}$$

where $v_1$, $v_{g1}$, $v_{g2}$ and $v_2$ are the spatial regions where the corresponding potentials are acting. These regions are about to be revealed further on.

## 4. MATCHING POTENTIAL SURFACES

One of the most important issues for the two-center shell models is that the separation plane between the two fragments is not the one where the potentials equal each other. As an example, for compact shapes (no neck, $R_3 = 0$) the points $(\{\rho_s, z_s\})$ on the separation line (where the two ellipsae intersect) result in different values for the potentials, $V_1(\rho_s, z_s) \neq V_2(\rho_s, z_s)$. The sharp cusp between the two values makes calculation totally wrong. Attempts to solve the problem by a geometrical transition function, making the frequency $\omega_{\rho_1}(z)$ join $\omega_{\rho_2}(z)$, introduce an unpredictable approximation which is bigger as the mass asymmetry is larger; moreover, it does not reproduce the neck spherical shape and still, only the $\rho$ – part of the potential is solved.

In conclusion, one has to divide the Hilbert space such that the *whole* potential $V_{DTCSM}(\rho, z)$ could smoothly and continuously pass from one fragment to the neck and finally to the other fragment.

First, let us take the deformed fragment oscillators into consideration and find out what are the spatial limits of continuity between the two potentials. The equation for such a region must be complacent with the matching condition:

$$V_1(\rho, z) = V_2(\rho, z) \tag{19}$$

where

$$\begin{aligned} V_1 &= \frac{1}{2} m_0 \omega_{\rho_1}^2 \rho^2 + \frac{1}{2} m_0 \omega_{z_1}^2 (z + z_1)^2 \quad , S_1(\rho, z) \\ V_2 &= \frac{1}{2} m_0 \omega_{\rho_2}^2 \rho^2 + \frac{1}{2} m_0 \omega_{z_2}^2 (z - z_2)^2 \quad , S_2(\rho, z) \end{aligned} \tag{20}$$

or

$$\omega_{\rho_1}^2 \rho^2 + \omega_{z_1}^2 (z + z_1)^2 = \omega_{\rho_2}^2 \rho^2 + \omega_{z_2}^2 (z - z_2)^2 \tag{21}$$

If one translates the $z-$coordinate:

$$z = z' - k \tag{22}$$

and separate the terms with respect to the powers of $\rho$ and $z'$, we get:

$$\begin{aligned} &(\omega_{\rho_1}^2 - \omega_{\rho_2}^2) + (\omega_{z_1}^2 - \omega_{z_2}^2) z'^2 - 2k(\omega_{z_1}^2 - \omega_{z_2}^2) z' + (\omega_{z_1}^2 - \omega_{z_2}^2) k^2 + \\ &+ 2(\omega_{z_1}^2 z_1 + \omega_{z_2}^2 z_2) z' - 2(\omega_{z_1}^2 z_1 + \omega_{z_2}^2 z_2) k + \omega_{z_1}^2 z_1^2 - \omega_{z_2}^2 z_2^2 = 0 \end{aligned} \tag{23}$$

We notice that:

$$z_1 + z_2 = R \tag{24}$$

and after some simple calculations one obtains:

$$\frac{\rho^2}{\frac{\omega_{z_1}^2 \omega_{z_2}^2 R^2}{(\omega_{\rho_2}^2 - \omega_{\rho_1}^2)(\omega_{z_2}^2 - \omega_{z_1}^2)}} + \frac{(z+k)^2}{\frac{\omega_{z_1}^2 \omega_{z_2}^2 R^2}{(\omega_{z_2}^2 - \omega_{z_1}^2)^2}} = 1 \tag{25}$$

which defines a so-called unique center surface, here namely an ellipsoid with semiaxes:

$$\begin{aligned} a_m &= \frac{\omega_{z_1} \omega_{z_2} R}{\omega_{z_2}^2 - \omega_{z_1}^2} \\ b_m &= \frac{\omega_{z_1} \omega_{z_2} R}{[(\omega_{\rho_2}^2 - \omega_{\rho_1}^2)(\omega_{z_2}^2 - \omega_{z_1}^2)]^{\frac{1}{2}}} \end{aligned} \tag{26}$$

Since the origin of this surface is at $(\rho = 0,\ z' = 0)$, its center with respect to the arbitrary origin (against which the potentials are expressed) is on the symmetry axis at:

$$z_{0m} = k = \frac{a_2^2 z_1 + a_1^2 z_2}{a_1^2 - a_2^2} \tag{27}$$

What we have obtained are the coordinates $(z_{0m}, 0)$ and the semiaxes $(a_m, b_m)$ of a matching potential ellipsoid (MPE). On its surface $V_1(\rho, z) = V_2(\rho, z)$. The heavy deformed fragment $O_1$ is acting through $V_1(\rho, z)$ outside the MPE. The light fragment part which emerges from the parent is contained inside MPE. Hence its action on the Hilbert space, $V_2(\rho, z)$, goes all over the matching ellipsoid volume.

The same demonstration is valid for $V_1(\rho, z) = V_{g1}(\rho, z)$, and $V_2(\rho, z) = V_{g2}(\rho, z)$, as far as the neck potential shares its action space with the fragments. First condition:

$$V_1(\rho, z) = V_{g1}(\rho, z) \tag{28}$$

or

$$\frac{1}{2} m_0 \omega_{\rho_1}^2 \rho^2 + \frac{1}{2} m_0 \omega_{z_1}^2 (z + z_1)^2 = 2V_0 - \left[ \frac{1}{2} m_0 \omega_g^2 (\rho - \rho_3)^2 + \frac{1}{2} m_0 \omega_g^2 (z - z_3)^2 \right] \tag{29}$$

yields:

$$(m_0\omega_{\rho_1}^2 + m_0\omega_g^2)\rho^2 + (m_0\omega_{z_1}^2 + m_0\omega_g^2)z^2 - 2m_0\omega_g^2\rho_3\rho + \\ + 2(m_0\omega_{z_1}^2 z_1 - m_0\omega_g^2 z_3)z + m_0\omega_{z_1}^2 z_1^2 + m_0\omega_g^2(\rho_3^2 + z_3^2) - 4V_0 = 0 \tag{30}$$

This equation is of the type:

$$a_{11}\rho^2 + a_{22}z^2 + 2a_1\rho + 2a_2 z + a = 0 \tag{31}$$

To describe a unique center surface, the normalized determinant of the equation:

$$\frac{\Delta}{\delta} = a - \frac{a_1^2}{a_{11}} - \frac{a_2^2}{a_{22}} \tag{32}$$

must be positive, which is the case for our situation. Then the center of the surface has the coordinates:

$$\rho_{0m1} = \frac{\begin{vmatrix} a_{12} & a_1 \\ a_{22} & a_2 \end{vmatrix}}{\begin{vmatrix} a_{11} & a_{12} \\ a_{21} & a_{22} \end{vmatrix}} \qquad z_{0m1} = -\frac{\begin{vmatrix} a_{11} & a_1 \\ a_{21} & a_2 \end{vmatrix}}{\begin{vmatrix} a_{11} & a_{12} \\ a_{21} & a_{22} \end{vmatrix}} \tag{33}$$

After some simple calculations one obtains:

$$\rho_{0m1} = \frac{\omega_g^2\rho_3}{\omega_{\rho_1}^2 + \omega_g^2} \qquad z_{0m1} = \frac{\omega_g^2 z_3 - \omega_{z_1}^2 z_1}{\omega_{z_1}^2 + \omega_g^2} \tag{34}$$

This surface is again an ellipsoid with semiaxes:

$$a_{m1} = \left(-\frac{\Delta}{\delta}\frac{1}{a_{22}}\right)^{1/2} \qquad b_{m1} = \left(-\frac{\Delta}{\delta}\frac{1}{a_{11}}\right)^{1/2} \tag{35}$$

and represents the matching potential ellipsoid (MPE1) between $V_1(\rho, z)$ and $V_{g1}(\rho, z)$. On its surface, the two values equal to each other. Obviously, the tangent point between this first matching potential ellipsoid and the heavy fragment shape is the same as the tangent point between the neck sphere and the heavy fragment. In the interior of MPE1, the DTCSM potential is $V_{g1}(\rho, z)$. Following the same arguments for:

$$V_2(\rho, z) = V_{g1}(\rho, z) \tag{36}$$

one finds:

$$\rho_{0m2} = \frac{\omega_g^2\rho_3}{\omega_{\rho_2}^2 + \omega_g^2} \qquad z_{0m2} = \frac{\omega_g^2 z_3 - \omega_{z_2}^2 z_2}{\omega_{z_2}^2 + \omega_g^2} \tag{37}$$

for the center of the second neck matching potential ellipsoid (MPE2), and the same expressions with $V_2(\rho, z)$ corresponding values instead of $V_1$ hold for the semiaxes $a_{m2}$ and $b_{m2}$.

What is achieved in this section is spanning the deformation space by DTCSM potential, passing continuously from the potential generated by the heavy fragment $V_1$ to the lighter one $V_2$ and allowing also for the neck to be smoothly shaped by $V_g$. There are no sharp cusps in the potential values. Since we work in axial symmetry, the two neck matching ellipsoids MPE1 and MPE2 are in fact rolling around the symmetry axis. Each of them shapes a thorus around the necking region, where $V_{g1}$ is the DTCSM potential.

## 5. DIAGONALIZATION BASIS

This section will browse succinctly the main steps to be taken in order to find a normalized functions set, since details about this issue have already been published [4].

The new feature in the DTCSM eigenvalue problem is the shape-dependency of the potentials: $V_{DTCSM}$, the spin-orbit term $V_{\mathbf{\Omega s}}$ and the $V_{\mathbf{\Omega}^2}$ term ($\mathbf{\Omega}$ is preferred here as a notation since the angular momentum operator, as being shape dependent, will be different from the usual $\mathbf{l}$). The total Hamiltonian:

$$H_{DTCSM} = -\frac{\hbar^2}{2m_0}\Delta + V_{DTCSM}(\rho, z) + V_{\mathbf{\Omega s}} + V_{\mathbf{\Omega}^2} \tag{38}$$

is obviously not separable. A basis is needed and diagonalization of oscillator potential differences and of angular momentum dependent operators has to be performed.

A separable Hamiltonian is obtained if one takes $\omega_{\rho_1} = \omega_{\rho_2} = \omega_1$, with no $\mathbf{ls}$ and $\mathbf{l}^2$ terms, hence a potential like:

$$V^{(d)}(\rho, z) = \begin{cases} V_1^{(d)}(\rho, z) = \frac{1}{2}m_0\omega_1^2\rho^2 + \frac{1}{2}m_0\omega_1^2(z+z_1)^2, & z \le 0 \\ V_2^{(d)}(\rho, z) = \frac{1}{2}m_0\omega_1^2\rho^2 + \frac{1}{2}m_0\omega_2^2(z-z_2)^2, & z \ge 0 \end{cases} \tag{39}$$

This is an appropriate two-center potential for a sphere ($z \le 0$) intersected with a vertical spheroid. The origin ($z = 0$) is the intersection plane. As a result of variable separation, three known differential equations are obtained for harmonic functions, Laguerre polynomial and Hermite function dependent solutions [4].

Using continuity conditions for $z$-dependent functions and their derrivatives at $z = 0$, the normalization condition and equalizing the energy on the symmetry axis $E_z = \hbar\omega_1(\nu_1 + 0.5) = \hbar\omega_2(\nu_2 + 0.5)$, $z$-quantum numbers and normalization constants for the $z$-dependent eigenfunctions are calculated. The $\phi$ and $\rho$-dependent functions are straighforward calculated from the differential equations. The final result is:

$$\Phi_m(\phi) = \frac{1}{\sqrt{2\pi}} \exp(im\phi)$$

$$R_{n_\rho}^{|m|}(\rho) = \sqrt{\frac{2\Gamma(n_\rho + 1)\alpha_1^2}{\Gamma(n_\rho + |m| + 1)}} \exp\left(-\frac{\alpha_1^2\rho^2}{2}\right)(\alpha_1^2\rho^2)^{\frac{|m|}{2}} L_{n_\rho}^{|m|}(\alpha_1^2\rho^2) \tag{40}$$

$$Z_\nu(z) = \begin{cases} C_{\nu_1} \exp\left[-\dfrac{\alpha_1^2(z+z_1)^2}{2}\right] H_{\nu_1}[-\alpha_1(z+z_1)], & z < 0 \\ C_{\nu_2} \exp\left[-\dfrac{\alpha_2^2(z-z_2)^2}{2}\right] H_{\nu_2}[\alpha_2(z-z_2)], & z \geq 0 \end{cases}$$

where $\Gamma$ is the gamma function, $L_n^m$ is the $m$-order Laguerre polynomial, $C_1$ and $C_2$ the normalization constants, $\nu_1$, $\nu_2$ the quantum numbers along the symmetry axis, and $H_\nu$ is the Hermite function. We now have a basis for further calculations. The eigenvalues for the diagonalized Hamiltonian with the potential $V^{(d)}$ are the oscillator energy levels for sphere+spheroid system:

$$E_{osc}^{(d)} = \hbar\omega_1(2n_\rho + |m| + 1) + \hbar\omega_{z_1}(\nu_1 + 0.5) \tag{41}$$

At this point we have a useful basis for the calculation of $H_{DTCSM}$ matrix elements.

## 6. LEVEL SCHEMES AND SHELL EFFECTS

Ten shell scheme matrix elements have been calculated, which means a $440 \times 440$ matrix. After proper diagonalization, the levels are obtained.

First, DTCSM spectra are computed for the superheavy fission reaction channel $^{306}122 \rightarrow {}^{198}\mathrm{W} + {}^{108}\mathrm{Cd}$, with the nuclei deformations $\chi_{122} = 0.9$, $\chi_W = 1.$ and $\chi_{\mathrm{Cd}} = 0.83$. Semiaxes $a_i$ and $b_i$ are calculated from the corresponding deformation parameter $\beta_2$ for every fragment, and using the volume conservation condition ($\beta_2^{^{198}\mathrm{W}} = 0.$, $\beta_2^{^{108}\mathrm{Cd}} = 0.135$ [5]). The reduced distance between centers

is chosen to represent the elongation parameter of the shape: $(R-R_i)/(R_f-R_i)$, where $R_i$ is the distance between centers when the light emerging fragment is completely embeded in the parent nucleus, and $R_f = a_1 + a_2 + 2R_3$ represents the final distance between centers, when the neck sphere is aligned with the fragments.

Five level schemes are calculated for five different neck parameters: $R_3 = 0$; 1; 4; 7; 10 fm. The labels on the left of the first scheme correspond to the spherical level scheme, for $R_3 = 0$. The fact that levels do not converge for $p_{3/2}$, $d_{5/2}$, etc., is due to the slight deformation of the parent nucleus, which resulted from shell corrections calculations. Strong irregularities appear as $R_3$ increase, especially upon the states corresponding to higher energies. At intermediary stages of splitting $((R-R_i)/(R_f-R_i) \approx 0.4-0.6$ there is an increase in higher level energies. This is due to the fact that the region where $V_g(\rho, z)$ is active becomes larger in volume; it is the moment to remember Fig. 5, which shows that potential inside the *neck-controlled* thorus is higher than the $V_1(\rho, z)$ and $V_2(\rho, z)$.

When one goes towards total splitting, MPE1 and MPE2 intersect the Oz-axis; their volumes decrease, and the neck influence vanishes little by little. As a result, the total potential is lower and the levels decrease their energies at $(R-R_i)/(R_f-R_i) \approx 0.9-1$. This behaviour is more obvious as $R_3$ is larger, when also contribution from $V_{g2} = V_0$, *inside* the shape span a larger region. It can be concluded that the neck-radius degree of freedom becomes more influential upon the single-particle energies in the last part of the overlapping region.

A direct consequence of the variation of the neck parameter $R_3$ on microscopic behaviour of a fission process is depicted in Fig. 1.

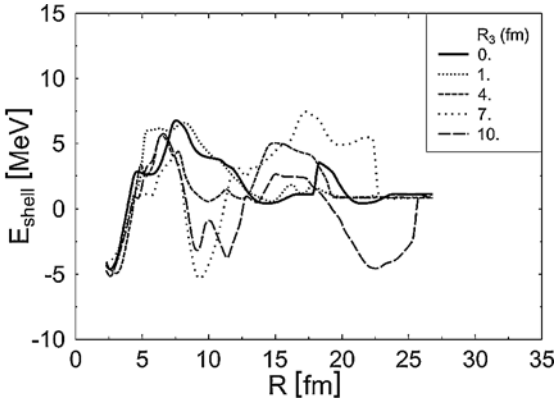


Fig. 1. – Neck influence on the shell corrections for different neck radii $R_3$ as a function of the distance between centers.

Here the shell corections are drawn for the five $R_3$ – parameter values, as a function of the distance between centers. They are calculated with the Strutinsky method. A shallow minimum at $R \approx 2.5$ fm suggests a small deformation of the $^{306}122$ ground state. First bump around $R \approx 5$–6 fm shows up in every case. Second bump is also there, but its position changes in $R$-value and in height (between $R = 12$ fm and $R = 20$ fm). The rather deep minimum ($\approx -5$ MeV) for large neck radii (apparent on the $R_3 = 10$ fm curve) is probably not manifested in $^{306}122$ fission, since at this distance between centers, the system is out of the fission barrier due to strong Coulombian repulsion.

## 7. CONCLUSIONS

The deformed two-center shell model presented in this work describes the evolution of single particle levels from one parent potential well to the two fragments.

The introduction of fragment ellipsoidal deformation in the two-center oscillator wells and further on, in the spin-orbit and $\mathbf{l}^2$ operators enables a more realistic calculation of the two interacting quantum systems. This new form of spin-orbit $\mathbf{\Omega s}$ and $\mathbf{\Omega}^2$ allows for the angular momentum dependent operators to follow the exact sequence of shapes throughout the splitting process. In such a way ellipsoidal degrees of freedom are considered within spin-orbit interaction.

The new necking-in dependent microscopic potential results in considering the neck degree of freedom into the level scheme calculation. As has been shown, the last part of the fision process is influenced by the difference in neck radii. This fact has important consequences on the potential barriers and fission paths on a potential energy surface calculated within more deformation degrees of freedom, necking included.

A new way of treating two partially overlapping nuclei has been introduced by making use of matching potential surfaces. It is only in this way that *continuity* between different regions of potential influence is assured. The potential passes smoothly from $V_1$ to $V_g$, to $V_2$ and so on without any cusp in its value and without the introduction of arbitrary geometric transition functions. For zero neck radius one obtains the fusion-like type of shapes.

All these facts make the presented model suitable for the study of fission channels and cluster decay phenomena and calculation of potential energy surfaces in fission.

Also the model provides the analysis of possible deformed target-projectile doors toward fusion processes in heavy ion reactions. In nucleus-nucleus collisions, calculations of two fusioning deformed partners yield the single particle spectra for the important (yet avoided up to now) region of overlapping shapes.

REFERENCES

1. D. N. Poenaru, M. Ivascu and W. Greiner, *Fission and Beta-Delayed Decay Modes*, vol. III, (CRC Press, Boca Raton, Florida, (1989); D. N. Poenaru and W. Greiner, *Nuclear Decay Modes* (Institute of Physics Publishing, Bristol, England, ch.6, (1996)).
2. R. A. Gherghescu, J. Skalski, Z. Patyk and A. Sobiczewski, Nucl. Phys., A**651**, 237 (1999).
3. W. I. van Rij and C. T. Hess, Nucl. Phys., A**142**, 72 (1970).
4. E. Badralexe, M. Rizea and A. Sandulescu, Rev. Roum. Phys., **19**, 63 (1974).
5. P. Moeller, J. R. Nix and K.-L. Kratz, Atomic Data Nucl. Data Tables **66**, 131 (1997).
6. A. C. Wahl, Atomic Data Nucl. Data Tables, **39**, 1 (1998).